

## Influence of Preparation Conditions on the Properties of Lithium Titanate Fabricated by a Solid-state Method

Guo-Qing Zhang<sup>1,2</sup>, Wenjuan Li<sup>1</sup>, Hongwei Yang<sup>1</sup>, Yahui Wang<sup>1</sup>, Sowjanya B. Rapole<sup>3</sup>, Yanli Cao<sup>1</sup>, Chunbao Zheng<sup>1</sup>, Keqiang Ding<sup>1,\*</sup> and Zhanhu Guo<sup>3,†</sup>

<sup>1</sup>College of Chemistry and Materials Science, Hebei Normal University, Shijiazhuang, Hebei 050024, P.R. China

<sup>2</sup>Faculty of Materials and Energy, Guangdong University of Technology, Guangzhou 510006, P. R. China

<sup>3</sup>Integrated Composites Laboratory (ICL), Dan F. Smith Department of Chemical Engineering, Lamar University, Beaumont, TX 77710, USA

Received: June 26, 2012, Accepted: August 23, 2012, Available online: September 24, 2012

**Abstract:** Lithium titanate ( $\text{Li}_4\text{Ti}_5\text{O}_{12}$ ) was prepared by a quasi solid-state method using water and ethanol as the solvents, in which  $\text{Li}_2\text{CO}_3$  and  $\text{TiO}_2$  were used as the starting materials. In this work, the calcination temperature, molar ratio of Li to Ti, and sintering time were all well investigated. The obtained samples were thoroughly characterized by XRD and SEM, revealing that the above three factors not only affected the crystal structure, but also the morphologies of the resultant samples. Galvanostatic charge discharge curves were also employed to evaluate the electrochemical performance of the samples. The best electrochemical performance of the samples was observed when the molar ratio of Li to Ti, sintering temperature and time are 6:5, 850 °C and 12 hours, respectively. It was revealed that the smaller particle size and the higher crystallinity of the resultant samples were favorable to enhance the electrochemical performance.

**Keywords:**  $\text{Li}_4\text{Ti}_5\text{O}_{12}$ ; solid-state method; sintering temperature; molar ratio; electrochemical performance

### 1. INTRODUCTION

Recently, rechargeable lithium-ion batteries with their light-weight and high energy density are gaining more attention because of their possible applications in high power devices such as hybrid electric vehicles [1, 2]. Therefore, research works on both cathode and anode materials have become an important task, especially for fundamental electrochemical researchers. Recently, it is revealed that when cathodes doped with transition metals such as Mn are combined with the currently commercialized carbon graphite anode, Mn reacted with  $\text{LiPF}_6$  electrolyte, and dissolved to form materials  $\text{MnF}$  [3], which can greatly degrade the electrochemical properties of the cells. In the lithium-ion batteries, for the most commonly used electrochemical couple of graphite/ $\text{LiCoO}_2$ ,  $\text{LiCoO}_2$  plays the role of the positive electrode (cathode) and graphite acts as the negative electrode (anode). At full charge, the highly lithiated graphite ( $\text{LiC}_6$ ) electrode is highly reactive because it operates close to the potential of metallic lithium [4]. Thus, lithium

plating and dendrite formation may occur, which in turn leads to the risk of internal short circuits [5]. To resolve these problems, various classes of anode materials known as transition metal oxides ( $\text{MoO}_2$ ,  $\text{CuO}$ ,  $\text{FeO}$  and  $\text{Li}_4\text{Ti}_5\text{O}_{12}$ ) have been investigated. Compared with other anode materials, except for low cost and non-toxicity, lithium titanate ( $\text{Li}_4\text{Ti}_5\text{O}_{12}$ ) has the following advantages, (1)  $\text{Li}_4\text{Ti}_5\text{O}_{12}$  spinel structure accommodates Li ions without changing the lattice constants of the cubic unit cell, showing long life cycles of hundreds or thousands [6]; (2)  $\text{Li}_4\text{Ti}_5\text{O}_{12}$  exhibits a flatter operation potential plateau and higher operating voltage of about 1.55 V versus  $\text{Li/Li}^+$ , which can entirely resolve the issue of lithium dendrite deposition on the surface of anode material [7]. Generally, there are two typical methods to fabricate  $\text{Li}_4\text{Ti}_5\text{O}_{12}$ . (a) A solid-state method, for example, Huang and co-workers [8] have synthesized Ag-doped  $\text{Li}_4\text{Ti}_5\text{O}_{12}$  at 850 °C by a solid-state reaction using  $\text{TiO}_2$ ,  $\text{Li}_2\text{CO}_3$  or  $\text{LiOH}$  as the starting materials, where the size of the as-prepared particles was close to 900 nm. Qi et al. [9] prepared Br-doped  $\text{Li}_4\text{Ti}_5\text{O}_{12}$  via a solid state reaction, in which  $\text{LiOH}\cdot\text{H}_2\text{O}$ ,  $\text{LiBr}\cdot\text{H}_2\text{O}$ , and  $\text{TiO}_2$  were used as the starting materials with the Li to Ti molar ratio of 4.35:5 and the resultant particle

To whom correspondence should be addressed:

\*Email: dkeqiang@263.net, Phone: +86-311-86268311; Fax: +86-311-86269217

†Email: zhanhu.guo@lamar.edu, Phone: (409) 880-7654/7195; Fax: (409) 880-2197

size was 1-2  $\mu\text{m}$ . (b) A sol-gel method, for instance, Zhang et al. [10] reported the synthesis of  $\text{Li}_4\text{Ti}_5\text{O}_{12}$  particles with sizes ranging from 90 to 110 nm, in which a kind of nonionic surfactant tri-block copolymer was employed as the chelating agent, and titanate isopropoxide and  $\text{Li}(\text{AC})_2 \cdot 2\text{H}_2\text{O}$  were utilized as the Ti source and Li resource, respectively.

Although many reports on the preparation of  $\text{Li}_4\text{Ti}_5\text{O}_{12}$  have been published, the detailed investigation on the influence of preparation conditions, such as the calcination temperature, molar ratio of Li to Ti, etc., on the properties of  $\text{Li}_4\text{Ti}_5\text{O}_{12}$  has not been reported. In the present work, the calcination temperature, sintering time and molar ratio of Li to Ti were probed systematically. Lastly, the optimum preparation conditions for fabricating  $\text{Li}_4\text{Ti}_5\text{O}_{12}$  were presented, and based on the charge-discharge cycle performance the importance of above three factors in affecting the electrochemical performance of obtained samples was found to follow a decreasing order in the manner of: molar ratio, calcination period, and sintering temperature.

## 2. EXPERIMENTAL

### 2.1. Materials

$\text{Li}_2\text{CO}_3$ ,  $\text{TiO}_2$  and other used reagents were all purchased from Tianjin Chemical Reagent Co. Ltd (China). All materials used in the electrochemical measurement, such as acetylene black, polytetrafluoroethylene (PTFE) binder, electrolyte of 1 M  $\text{LiClO}_4$  and the cell were all supported by the Tianjin Lianghuo S&T Developing Co. Ltd. All the chemicals were used as-received without any further treatment.

### 2.2. Preparation of $\text{Li}_4\text{Ti}_5\text{O}_{12}$

Due to the simplicity, a solid-state method was employed to fabricate  $\text{Li}_4\text{Ti}_5\text{O}_{12}$ . Briefly,  $\text{Li}_2\text{CO}_3$  and  $\text{TiO}_2$  (The molar ratios of Li to Ti are 4:5, 6:5, and 8:5, respectively) were mixed by a magnetic mixer using distilled water having ethanol (the volume ratio of water to ethanol is 7:3) as the solvent. Then in a desiccator the resultant mixture was dried at 80  $^\circ\text{C}$  for around 5 hours to form a dried precursor. The well ground precursors were heated in a muffle furnace at desired temperatures for various periods. After cooling down to room temperature,  $\text{Li}_4\text{Ti}_5\text{O}_{12}$  particles were prepared.

### 2.3. Characterization, Electrode Preparation and Electrochemical Testing

X-ray diffraction (Bruker AXS, D8 ADVANCE, Germany) was used to examine the phase homogeneity. The particle morphology was observed by scanning electron microscopy (HITACHI, SEM S-570). Fourier transform infrared spectrometry (FT-IR) measurements were carried out on a Hitachi FT-IR-8900 spectrometer (Japan).

The cathodes used for the electrochemical characterization were fabricated by blending the prepared active material powders with acetylene black and polytetrafluoroethylene (PTFE) binder in a weight ratio of 85:10:5. Two-electrode electrochemical cells consisting of lithium metal foil as the negative electrode, Celgard 2400 separator, and an electrolyte of 1 M  $\text{LiClO}_4$  in ethylene carbonate (EC):diethyl carbonate (DEC):dimethyl carbonate (DMC) (2:5:11, vol.) were assembled in a nitrogen-filled glove box. The electrochemical cycle tests were performed using a LAND series battery testing system (Wuhan Kinguo Electronics Co., Ltd. China) at vari-

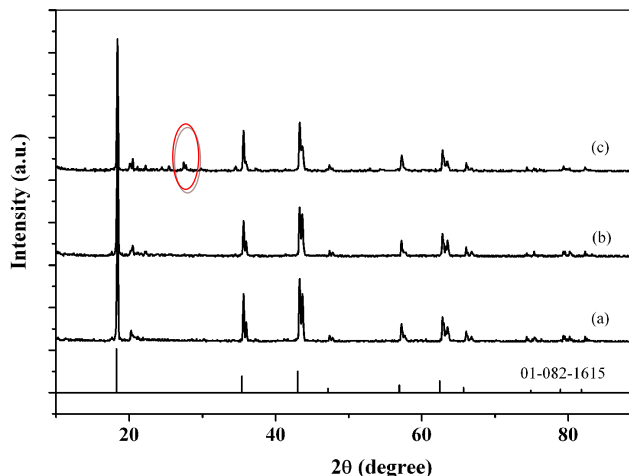


Figure 1. XRD patterns of  $\text{Li}_4\text{Ti}_5\text{O}_{12}$  prepared at temperature of (a) 750, (b) 850, and (c) 950  $^\circ\text{C}$ .

ous rates (1 C=175 mAh/g) [9] between 0.5 and 2.5 V at room temperature. The impedance measurements were carried out at open circuit potential with an applied 10 mV sinusoidal perturbation in a  $10^5$  Hz down to 0.1 Hz frequency range with 10 steps per decade at room temperature.

## 3. RESULTS AND DISCUSSION

### 3.1. The influence of calcination temperature on the properties of $\text{Li}_4\text{Ti}_5\text{O}_{12}$

Fig. 1 shows the XRD patterns of the prepared samples, in which the calcination temperatures were different from each other. In the preparation process, the molar ratio of Li to Ti and the sintering time are kept to be 1:2 and 12 hours, respectively. It can be seen that compared to the standard XRD patterns of  $\text{Li}_4\text{Ti}_5\text{O}_{12}$  (JCPDS card No. 01-082-1615), the main diffraction peaks are clearly displayed in all XRD patterns, suggesting that the main phase in the resultant samples was  $\text{Li}_4\text{Ti}_5\text{O}_{12}$ . Unfortunately, a small peak appearing at around  $2\theta = 20.56^\circ$  was found in all XRD patterns. It indicated that a trace amount of  $\text{Li}_2\text{TiO}_3$  [11] was contained in the as-prepared samples. For the sample prepared at 950  $^\circ\text{C}$ , i.e., pattern c, as shown by the circled part, a small diffraction peak located at  $2\theta = 27^\circ$  is displayed, which can be assigned to rutile- $\text{TiO}_2$  [11]. Also, One can see that some blurry-shaped peaks are exhibited in pattern a, namely, for the samples sintered at 750  $^\circ\text{C}$ . That is to say, more impurities were fabricated when the calcination temperature is as low as 750  $^\circ\text{C}$ . Thus, among the three kinds of samples, the sample prepared at 850  $^\circ\text{C}$  has the best crystal structure, which may promise its better electrochemical performance.

SEM images for the as-prepared are clearly shown in Fig.2. The morphologies of samples shown in Fig.2 were rather similar to that reported by Kim[12], in which  $\text{Li}_4\text{Ti}_5\text{O}_{12}$  nanoparticles were precipitated from ethylene glycol solution of titanium tetra isopropoxide ( $\text{Ti}(\text{O}-i\text{Pr})_4$ ) and  $\text{Li}_2\text{O}_2$ . One can see that the particle size of the resultant samples was greatly affected by the sintering temperature, though the morphologies of the samples were not much altered by the calcination temperatures. The particle sizes for the samples prepared at 750  $^\circ\text{C}$ , 850  $^\circ\text{C}$  and 950  $^\circ\text{C}$  are around 650nm, 450nm

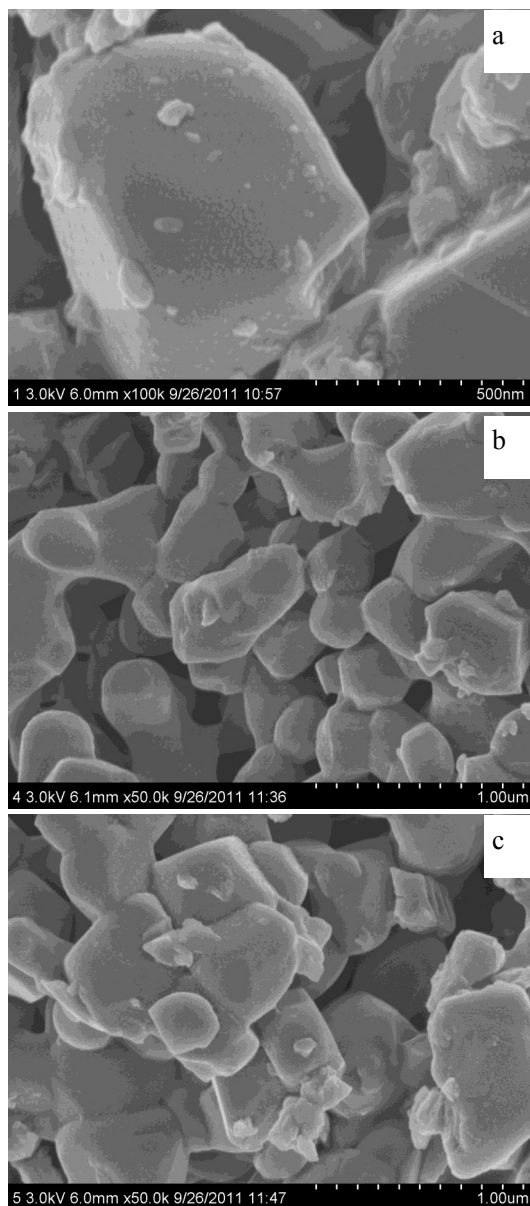


Figure 2. SEM images of  $\text{Li}_4\text{Ti}_5\text{O}_{12}$  prepared at temperature of (a) 750, (b) 850 and (c) 950 °C.

and 910nm, respectively. Moreover, compared with those particles prepared at 750°C and 950 °C, the particles fabricated at 850 °C showed a more uniform distribution of particle size. As reported by Gaberscek [13] et al., the smaller size favors the intercalation/de-intercalation process of the Li ions and the discharge capacity drops more or less linearly with increasing particle size. Thus, the  $\text{Li}_4\text{Ti}_5\text{O}_{12}$  prepared at 850 °C may have better electrochemical performance compared with the other two samples.

Fig. 3 shows the IR spectra for the as-prepared  $\text{Li}_4\text{Ti}_5\text{O}_{12}$ . The two absorption bands centered at 644.1 and 453.2  $\text{cm}^{-1}$ , respectively, are due to the symmetric and asymmetric stretching vibrations of the octahedral groups  $[\text{MO}_6]$  lattice [14]. The wide and strong peak at 3700–2500  $\text{cm}^{-1}$  (hydrogen-bonded O-H stretching)

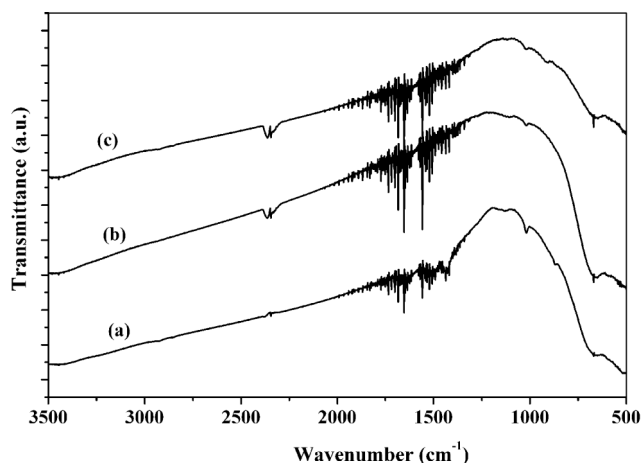


Figure 3. FT-IR spectra of  $\text{Li}_4\text{Ti}_5\text{O}_{12}$  prepared at temperature of (a) 750, (b) 850 and (c) 950 °C

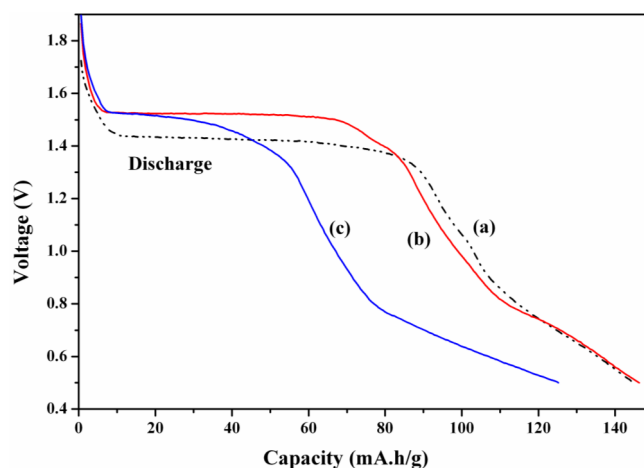


Figure 4. Discharge curves at 0.2 C of the cells assembled by the  $\text{Li}_4\text{Ti}_5\text{O}_{12}$  prepared at temperature of (a) 750, (b) 850, (c) 950 °C.

indicates the existence of O-H bonds in the structure which is consistent with the hypothetical formula [15]. The 1516, 1440 and 866  $\text{cm}^{-1}$  peaks could be assigned to  $\text{CO}_3^{2-}$  species, for samples can react with  $\text{H}_2\text{O}$  and  $\text{CO}_2$  to yield carbonate like  $\text{Li}_2\text{CO}_3$  when exposed to the atmosphere. And the peak at 652  $\text{cm}^{-1}$  could be the absorption of stretching Ti-O bond [16]. Since the FTIR spectra shown in Fig.3, especially in the lower wavenumber region, are very similar to the reported IR spectra of  $\text{Li}_4\text{Ti}_5\text{O}_{12}$  [16], it can be concluded that the main content in the samples is  $\text{Li}_4\text{Ti}_5\text{O}_{12}$ . This result is consistent with that obtained from XRD patterns in Fig.1 very well.

The discharge capacities of the cells assembled by  $\text{Li}_4\text{Ti}_5\text{O}_{12}$  prepared at various temperatures were also evaluated, as illustrated in Fig. 4. It can be seen that in the potential range from 2.5 to 0.5V vs Li/Li+, the discharge capacities at 0.2C for samples fabricated at 750 °C, 850 °C and 950 °C are 144, 148, 125 mAh/g, respectively. For the sample of  $\text{Li}_4\text{Ti}_5\text{O}_{12}$  prepared at 750 °C, as shown by curve

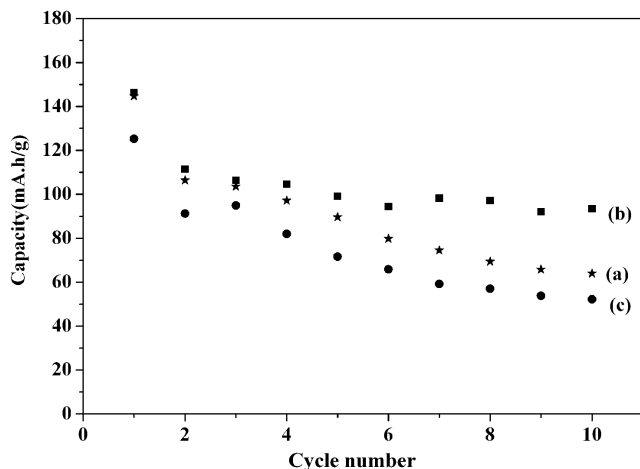


Figure 5. Charge-discharge cycle performances of the LTO samples prepared at temperature of (a) 750, (b) 850, and (c) 950 °C.

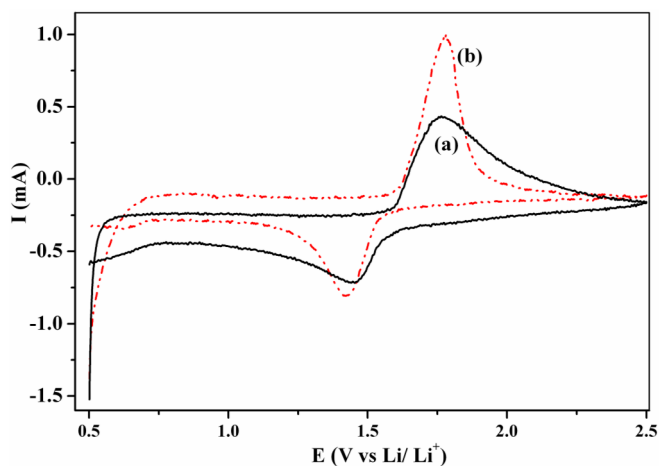


Figure 6. Cyclic voltammograms (CVs) of the cells assembled by the LTO prepared at temperature of (a) 850 and (b) 750 °C.

a, the discharge voltage plateau is at around 1.437V, lower than the voltage plateau of around 1.525V for curve b and c. Generally, when the discharging rate is increased, the discharging voltage plateau would shift in the negative-direction [8], indicating that the polar potential will increase with the increased current density. In other words, the lower discharging capacity platform, as showed in curve a, may correspond to a higher polarization overpotential, compared with curves b and c. That is to say, the cell corresponding to curve a may have a larger charge transfer resistance compared with the other two cells when discharged at the same rates. Also, one can see that the discharging voltage plateau of curve c was shorter than that of curve b. The discharging potential plateau corresponds to a two-phase transformation, and a longer platform indicated a larger amount of active material taking part in the intercalation/de-intercalation process of the Li ions. Therefore, it seemed that the mass percentage of  $\text{Li}_4\text{Ti}_5\text{O}_{12}$  in the sample prepared at 850 °C was larger than that prepared at 950 °C. In conclu-

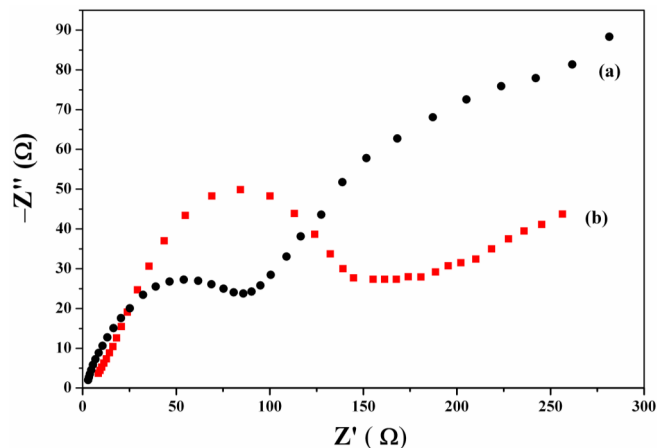


Figure 7. Nyquist plots of the cells assembled by the LTO prepared at temperature of (a) 850 and (b) 750 °C.

sion, the electrochemical behavior, i.e., the discharge voltage plateau and discharge capacity, exhibited by  $\text{Li}_4\text{Ti}_5\text{O}_{12}$  prepared at 850 °C is superior to the other two samples prepared at 750 °C and 950 °C. However, we do admit the discharge capacity reported here is not the best one compared with the published data. For example, Hsiao's group [17] reported that the dense- $\text{Li}_4\text{Ti}_5\text{O}_{12}$  can deliver 165mAh/g at 0.2 discharging rate.

The cycle performance of the cells was also considered, as shown in Fig.5. It can be seen that with the increase of cycle number, the discharge capacity decreased dramatically. After 10 cycles, the discharge capacities for the cells assembled by  $\text{Li}_4\text{Ti}_5\text{O}_{12}$  fabricated at 750 °C, 850 °C and 950 °C changed from 144, 148 and 125 to 64, 93 and 53 mAh/g, respectively. This result strongly demonstrates that the sample prepared at 850 °C showed the best electrochemical performance among the three samples, due to its smaller particle size and higher crystalline structure.

It is widely known that the shapes of redox peaks observed in a CV curve can reflect the electrochemical reaction kinetics of  $\text{Li}^+$  insertion/deinsertion. Thus, cyclic voltammograms (CVs) of the cells assembled by the as-prepared  $\text{Li}_4\text{Ti}_5\text{O}_{12}$  were also conducted as shown in Fig.6. It can be seen that well-defined CVs were displayed by the cells, indicating that the intercalation/de-intercalation process of the Li ions can proceed freely in the cells. For curve a, the anodic and cathodic peak potentials are located at 1.764V and 1.453V, respectively. And the potential interval ( $\Delta E_p = E_{pa} - E_{pc}$ ) is close to 311mV, while for curve b, corresponding to the sample prepared at 750 °C, the anodic and cathodic peak potentials are located at 1.782V and 1.420V, respectively, and the potential interval ( $\Delta E_p = E_{pa} - E_{pc}$ ) is close to 362mV. Generally, the smaller potential separation corresponds to a more reversible redox process [18]. Thus, it can be inferred from Fig.6 that the reversibility of the intercalation/de-intercalation process of Li ions in  $\text{Li}_4\text{Ti}_5\text{O}_{12}$  prepared at 850 °C is superior to that fabricated at 750 °C, though the peak currents, including anodic and cathodic peak current, exhibited by curve a, are smaller than that showed by curve b.

Nyquist plots, one type of curves in Electrochemical Impedance Spectroscopy (EIS), is a main method for evaluating the electrochemical performance of cells. Nyquist plots for the cells assem-

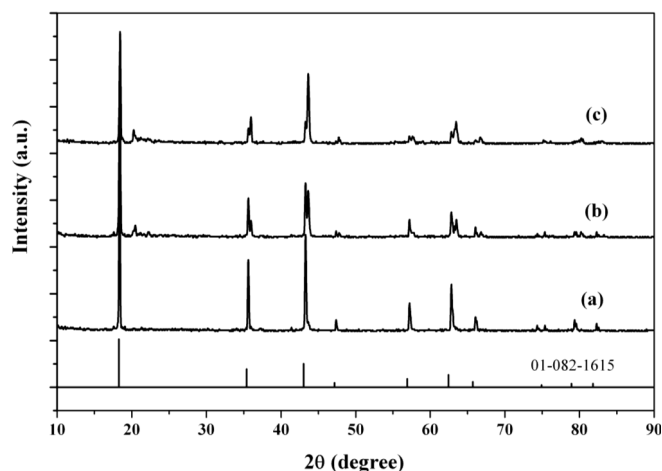


Figure 8. XRD patterns of  $\text{Li}_4\text{Ti}_5\text{O}_{12}$  prepared at  $850\text{ }^\circ\text{C}$  with molar ratio of (a) 4:5, (b) 6:5 and (c) 8:5.

bled by our samples were conducted as illustrated in Fig. 7. One can see that the impedance spectra of the cells showed an intercept at high frequency, followed by a semicircle in the high-middle frequency region, and a straight line in the low frequency region, according with the published figure very well [7]. Generally, it is regarded [19] that the intercept impedance on the  $Z_{\text{real}}$  axis represents the ohmic resistance, which consists of the resistance of the electrolyte and electrode. The high-frequency region of the semicircle represents the migration of the  $\text{Li}^+$  ions at the electrode/electrolyte interface through the solid electrolyte interface (SEI) layer, whereas the middle frequency range of the semicircle corresponds to the charge-transfer process. The low frequency region of the straight line is attributed to the diffusion of the lithium ions into the bulk of the electrode material or so called Warburg diffusion. Thus, approximately, the diameter of the semicircle appearing in the high-middle frequency region stands for the value of charge transfer resistance ( $R_{\text{ct}}$ ). The charge transfer resistances for the cells assembled by  $\text{Li}_4\text{Ti}_5\text{O}_{12}$  prepared at  $850\text{ }^\circ\text{C}$  and that at  $750\text{ }^\circ\text{C}$  were estimated to be around 125 and 165  $\Omega$ , respectively. It proved that the electrochemical performance displayed by  $\text{Li}_4\text{Ti}_5\text{O}_{12}$  prepared at  $850\text{ }^\circ\text{C}$  should be better than the kind of  $\text{Li}_4\text{Ti}_5\text{O}_{12}$  prepared at  $750\text{ }^\circ\text{C}$ , which can strongly explain the results showed in Fig. 4, namely, both the discharge capacity and cycle performance of  $\text{Li}_4\text{Ti}_5\text{O}_{12}$  prepared at  $850\text{ }^\circ\text{C}$  excelled that exhibited by the sample prepared at  $750\text{ }^\circ\text{C}$ .

### 3.2. The influence of molar ratio of Li to Ti on the properties of $\text{Li}_4\text{Ti}_5\text{O}_{12}$

Fig. 8. shows the XRD patterns of the prepared samples, in which the molar ratio of Li to Ti are different from each other. The sintering temperature and time are fixed to be  $850\text{ }^\circ\text{C}$ , 12 hours, respectively. One can see that the main diffraction peaks of spinel structure of  $\text{Li}_4\text{Ti}_5\text{O}_{12}$  are clearly displayed by all patterns, suggesting that the main content of the as-prepared samples are  $\text{Li}_4\text{Ti}_5\text{O}_{12}$ . When the molar ratio of Li to Ti is 8:5, as shown by pattern **c**, compared with patterns **a** and **b**, wider diffraction peaks were displayed. It indicates that the crystallinity of  $\text{Li}_4\text{Ti}_5\text{O}_{12}$  corresponding

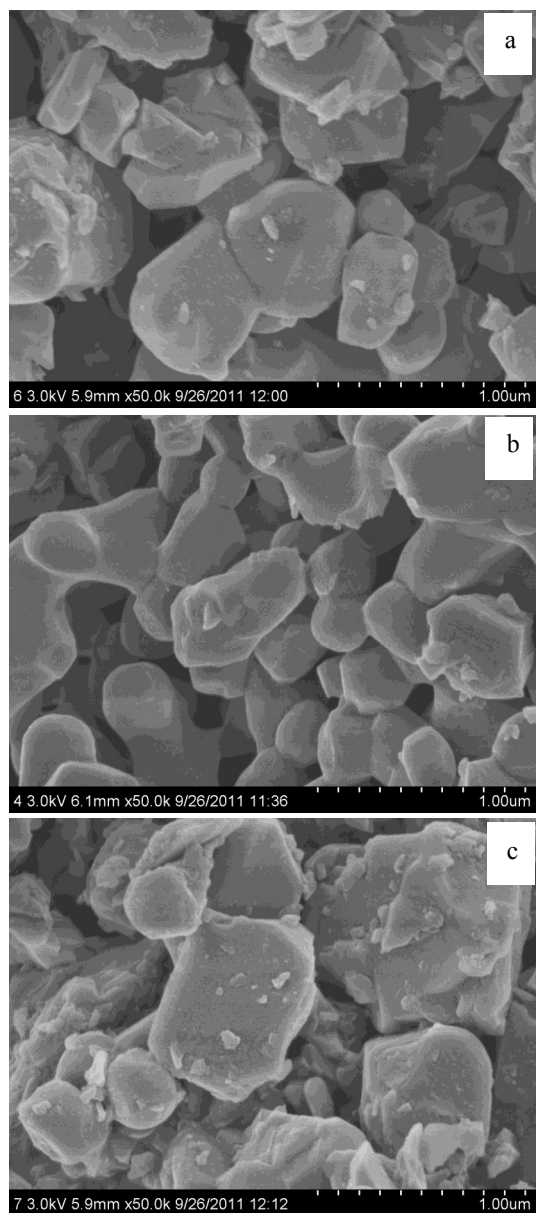


Figure 9. SEM microstructures of  $\text{Li}_4\text{Ti}_5\text{O}_{12}$  prepared at  $850\text{ }^\circ\text{C}$  with molar ratio of (a) 4:5, (b) 6:5 and (c) 8:5.

to pattern **c** is inferior to the other two samples [20]. Owing to the volatilization of Li in the preparation process [9], the molar ratio of Li to Ti of 6:5 was thought as the best value employed for fabricating  $\text{Li}_4\text{Ti}_5\text{O}_{12}$ .

SEM images for the samples, prepared at various molar ratios, are clearly shown in Fig. 9. It can be seen that some irregular particles were decorated on the surface of regular particles when the molar ratio of Li to Ti is 4:5. Interestingly, at the molar ratio of 6:5, only regular particles can be observed, while, at the molar ratio of 8:5, more irregular small particles were formed on the surface of regular particles, indicating that some unknown substances were formed in the preparation process. That is to say, excess amounts of Li in the starting materials are not favorable for preparing pure

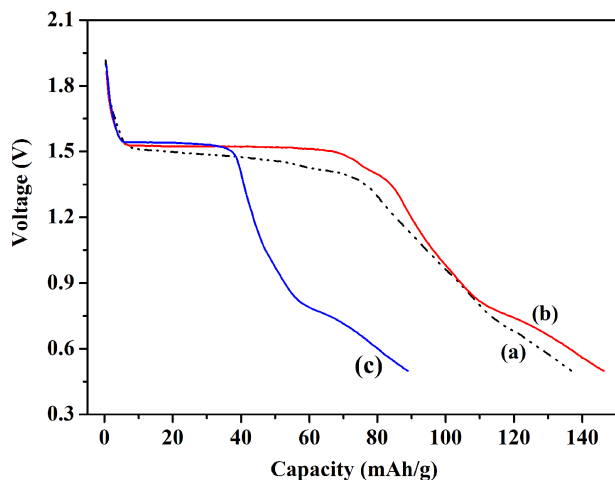


Figure 10. Discharge curves for the cells assembled by the  $\text{Li}_4\text{Ti}_5\text{O}_{12}$  prepared at 0.2C with a molar ratio of (a) 4:5, (b) 6:5 and (c) 8:5.

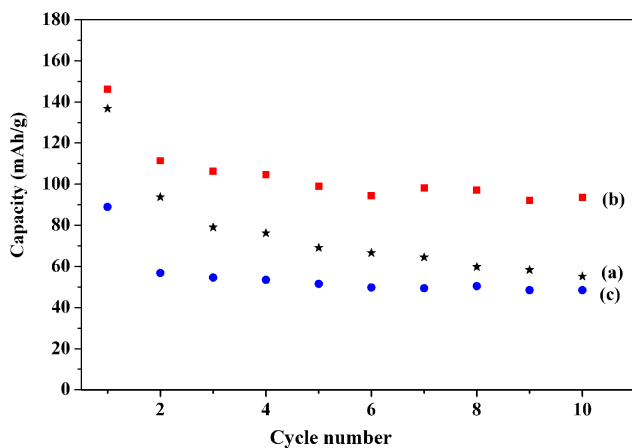


Figure 11. Charge-discharge cycle performances of the LTO samples prepared at a Li to Ti molar ratio of (a) 4:5, (b) 6:5 and (c) 8:5.

$\text{Li}_4\text{Ti}_5\text{O}_{12}$  due to some formed impurities. Also, the particle sizes for the samples prepared at the molar ratios of 4:5, 6:5 and 8:5 were approximately estimated to be around 453~615nm, 456~460nm and 636~701nm, respectively, based on the SEM images obtained. Thus, the particle size of  $\text{Li}_4\text{Ti}_5\text{O}_{12}$  prepared at 6:5 was located at a very narrow range, which is favorable for the intercalation/deintercalation process of the Li ions due to the identical Li ion diffusion paths [21].

Fig.10 shows the discharge capacities of cells structured by the as-prepared  $\text{Li}_4\text{Ti}_5\text{O}_{12}$  at different molar ratios. It can be seen that the discharge capacities at 0.2C for samples fabricated at molar ratios of 4:5, 6:5 and 8:5 are 137, 148, 89 mAh/g, respectively. For the sample of  $\text{Li}_4\text{Ti}_5\text{O}_{12}$  prepared at 4:5, as shown by curve **a**, a sloped voltage plateau between 1.52 to 1.40V vs  $\text{Li}/\text{Li}^+$  was exhibited. The sloped voltage plateau can be attributed to the increased solid-solution region between the pristine and lithiated phases, resulting from the high surface or interface energies in nanosized

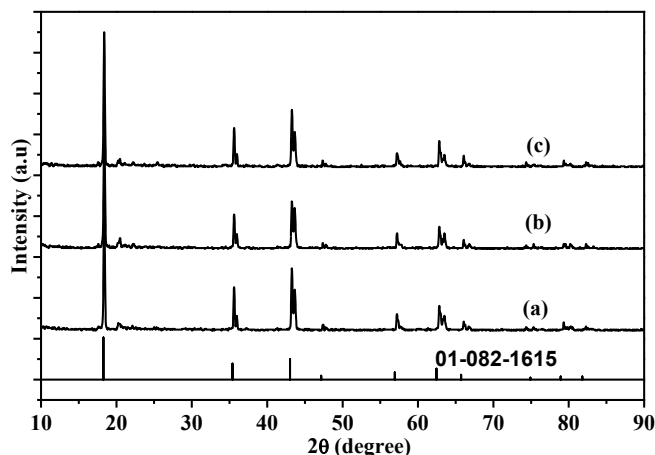


Figure 12. XRD patterns for  $\text{Li}_4\text{Ti}_5\text{O}_{12}$  prepared at various sintering periods of (a) 9 h, (b) 12 h, and (c) 15 h.

particles [22]. In other words, for the sample corresponding to curve **a**, a two-phase transformation reaction in charging-discharging was partially replaced by the solid-solution reaction. While for curve **b**, a longer and flat discharge voltage plateau was observed. The long discharging potential plateaus imply a transformation from a Li-poor to a Li-rich phase during Li insertion, as a flat voltage response is characteristic of a two-phase electrochemical reaction [23]. A short discharging potential plateau was displayed in curve **a**, indicating a smaller amount of  $\text{Li}_4\text{Ti}_5\text{O}_{12}$  can take part in the two-phase electrochemical reaction during Li insertion. Thus, it is concluded that the  $\text{Li}_4\text{Ti}_5\text{O}_{12}$  prepared at the molar ratio of 6:5 showed the best charge-discharge behavior among the three samples.

The cycle performance of the cells comprised by as-prepared  $\text{Li}_4\text{Ti}_5\text{O}_{12}$  was also measured, as shown in Fig.11. Similar to the results shown in Fig.5, with the increase of cycle number, the discharge capacity decreased dramatically. After 10 cycles, the discharge capacities for the cells assembled by  $\text{Li}_4\text{Ti}_5\text{O}_{12}$  fabricated at 4:5, 6:5 and 8:5 varied from 137, 148 and 89 to 55, 93 and 49mAh/g, respectively. This result strongly demonstrates that the sample prepared at the molar ratio of 6:5 showed the best electrochemical performance among the three samples, mainly due to its uniform and smaller particle size as shown in Fig.9 and the higher crystalline structure shown in Fig.8.

### 3.3. The influence of sintering time on the properties of $\text{Li}_4\text{Ti}_5\text{O}_{12}$

Calcining period is a key factor during which the crystal transformation can take place. Thus, the effect of sintering period on the preparation of  $\text{Li}_4\text{Ti}_5\text{O}_{12}$  was considered in this part. Fig. 12 shows the XRD patterns of the prepared samples, in which the calcining periods are varied. It should be mentioned that the molar ratio of Li to Ti and the sintering temperature were 6:5 and 850 °C, respectively. The main diffraction peaks, compared to the standard XRD pattern of  $\text{Li}_4\text{Ti}_5\text{O}_{12}$  are clearly displayed, indicating that the main phase in the resultant samples was  $\text{Li}_4\text{Ti}_5\text{O}_{12}$ . As shown by the circled part in Fig.12, the diffraction peak shown in pattern **a** is

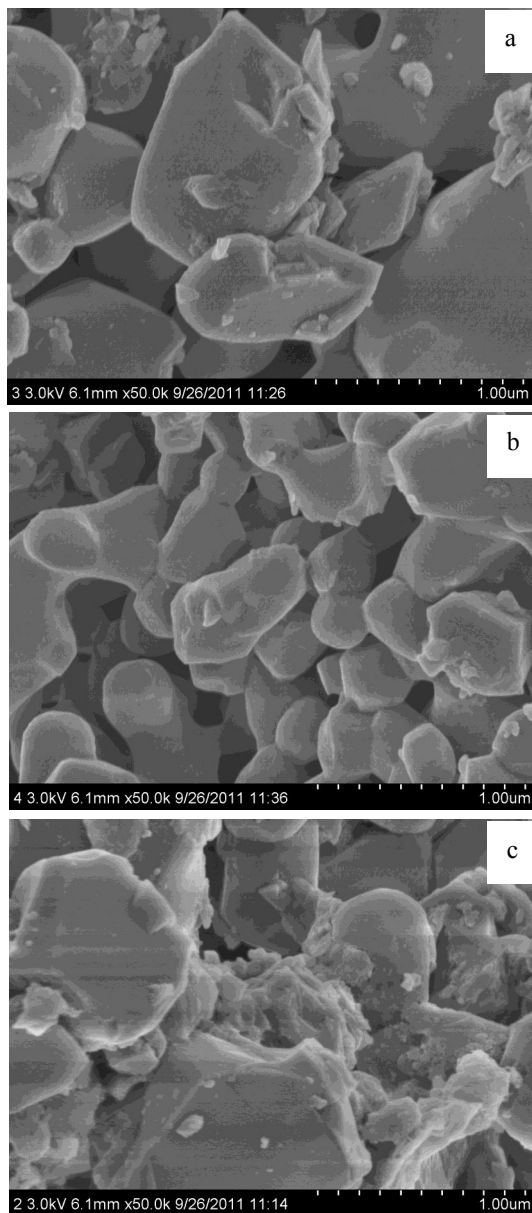


Figure 13. SEM images for  $\text{Li}_4\text{Ti}_5\text{O}_{12}$  prepared at various sintering periods of (a) 9 h, (b) 12 h, and (c) 15 h.

wider than that shown in pattern **b**. Thus, it can be concluded that with the increase of calcining period, samples with higher crystallinity were prepared. No more evident differences were found between patterns **b** and **c**. Thus, the calcining period of 12h was regarded as the best parameter for fabricating  $\text{Li}_4\text{Ti}_5\text{O}_{12}$ .

SEM images for the as-prepared samples are shown in Fig.13. Although no obvious differences were found in the XRD pattern, the morphologies are rather different from each other when the sintering periods are altered. Uniform particles, sizing at around 456nm, were observed when the sintering time was 12h. Particles, with a diameter close to 620nm, decorated with many irregular small particles were found when the sintering time was 9h. As the

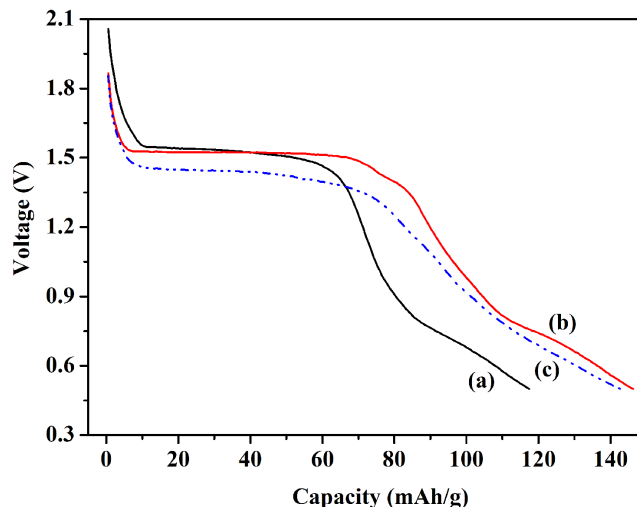


Figure 14. Discharge curves of the cells assembled by the  $\text{Li}_4\text{Ti}_5\text{O}_{12}$  prepared at 0.2C at various sintering periods of (a) 9 h, (b) 12 h, and (c) 15 h, respectively.

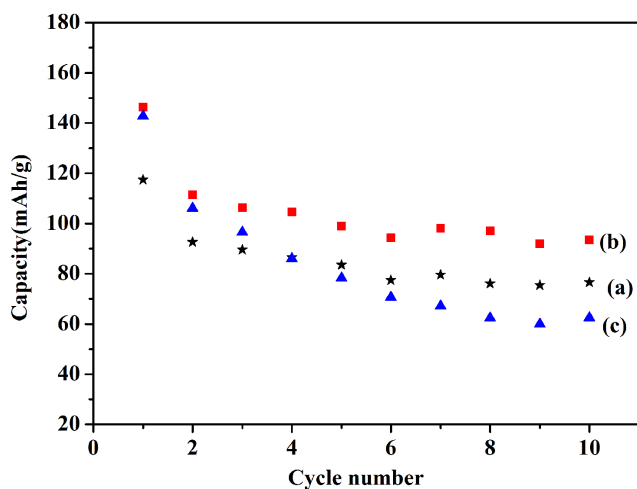


Figure 15. Charge-discharge cycle performances of LTO samples prepared at various sintering periods of (a) 9 h, (b) 12 h, and (c) 15 h, respectively.

calcining period reached 15h, larger particles with a diameter of greater than 900nm were observed. More importantly, when the sintering time was 15h, more irregular particles were created on the surface of the resultant larger particles.

The electrochemical performances of the cells assembled by  $\text{Li}_4\text{Ti}_5\text{O}_{12}$  prepared at various periods were also evaluated. Fig.14 shows the discharge capacities of all cells. It can be seen that in the potential range from 2.5 to 0.5V vs  $\text{Li}/\text{Li}^+$ , the discharge capacities at 0.2C for samples fabricated at 9h, 12h and 15h were 117, 146, 142 mAh/g, respectively. For the sample of  $\text{Li}_4\text{Ti}_5\text{O}_{12}$  prepared at 15h, the discharge voltage plateau is at around 1.44V, lower than the voltage plateau of at around 1.53V for curves **a** and **b**. As discussed above, the lower discharging voltage plateau may imply a

higher polar potential, which can hinder the intercalation/de-intercalation process of Li ions in  $\text{Li}_4\text{Ti}_5\text{O}_{12}$ . Compared to curve **b**, a shorter discharging voltage plateau was displayed in curve **a**. It indicates that the amount of active materials taking part in the intercalation/de-intercalation process of Li ions was lower than that of sample corresponding to curve **b**. Therefore, the electrochemical behavior, i.e., the discharge voltage plateau and discharge capacity, exhibited by  $\text{Li}_4\text{Ti}_5\text{O}_{12}$  prepared at 12h is superior to the other two samples prepared at 9h and 15h.

The cycle performance of the cells was also considered, as shown in Fig.15. With the increase of cycle number, the discharge capacity decreased obviously. After 10 cycles, the discharge capacities for the cells assembled by  $\text{Li}_4\text{Ti}_5\text{O}_{12}$  fabricated at 9h, 12h and 15h altered from 117, 148 and 142 to 77, 93 and 62mAh/g, respectively. This result strongly demonstrates that the sample prepared at 12h showed the best electrochemical performance among the three samples, mainly due to its uniform particle size distribution and pure phase.

#### 4. CONCLUSION

In this work, the influence of the calcination temperature, the molar ratio of Li to Ti, and the sintering time on the properties of as-prepared  $\text{Li}_4\text{Ti}_5\text{O}_{12}$  were all systematically investigated. It revealed that all the above three factors can greatly affect the particle sizes, the morphologies and the charging-discharging behaviors as well, of the resultant samples. The following conclusions are achieved. (1) Based on the initial discharging capacity, the importance of above factors are in the following order: molar ratio, calcining period, sintering temperature; (2) According to the SEM images and cycle performance shown in this work, uniform particle size and pure phase are thought as the key factors in determining the electrochemical performance. (3) The optimum preparation conditions are achieved, namely, the molar ratio of Li to Ti, sintering temperature and time of 6:5, 850 °C and 12h, respectively.

#### 5. ACKNOWLEDGEMENTS

This work was financially supported by the National Natural Science Foundation of China (No. 21173066), Natural Science Foundation of Hebei Province of China (No.B2011205014), Key Project Fund of Hebei Normal University (L2008Z08). Z.G. acknowledges the support from the U.S. National Science Foundation (Nanoscale Interdisciplinary Research Team and Materials Processing and Manufacturing) under Grant CMMI 10-30755.

#### REFERENCES

- [1] I. Hung, L. Zhou, F. Pourpoint, C.P. Grey, Z. Gan, *J. Am. Chem. Soc.*, 134, 1898 (2012).
- [2] A.M. Chockla, J.T. Harris, V.A. Akhavan, T.D. Bogart, V.C. Holmberg, C. Steinhagen, C. Buddie Mullins, K.J. Stevenson, B.A. Korgel, *J. Am. Chem. Soc.*, 133, 20914 (2011).
- [3] S. Komaba, B. Kaplan, T. Ohsuka, Y. Kataoka, N. Kumagai, H. Groult, *J. Power Sources*, 119, 378 (2003).
- [4] I. Belharouak, K. Amine, *Electrochem. Commun.*, 5, 435 (2003).
- [5] H. Schneider, P. Maire, P. Novák, *Electrochim. Acta*, 56, 9324 (2011).
- [6] H. Ge, N. Li, D. Li, C. Dai, D. Wang, *Electrochem. Commun.*, 10, 1031 (2008).
- [7] Y. Shi, L. Wen, F. Li, H.-M. Cheng, *J. Power Sources*, 196, 8610 (2011).
- [8] S. Huang, Z. Wen, X. Zhu, Z. Gu, *Electrochem. Commun.*, 6, 1093 (2004).
- [9] Y. Qi, Y. Huang, D. Jia, S.-J. Bao, Z.P. Guo, *Electrochim. Acta*, 54, 4772 (2009).
- [10] N. Zhang, Z. Liu, T. Yang, C. Liao, Z. Wang, K. Sun, *Electrochem. Commun.*, 13, 654 (2011).
- [11] D. Yoshikawa, Y. Kadoma, J.-M. Kim, K. Ui, N. Kumagai, N. Kitamura, Y. Idemoto, *Electrochim. Acta*, 55, 1872 (2010).
- [12] D.H. Kim, Y.S. Ahn, J. Kim, *Electrochem. Commun.*, 7, 1340 (2005).
- [13] M. Gaberscek, R. Dominko, J. Jamnik, *Electrochem. Commun.*, 9, 2778 (2007).
- [14] G.C. Allen, M. Paul, *Appl. Spectrosc.*, 49, 451 (1995).
- [15] V.M. Zainullina, V.P. Zhukov, T.A. Denisova, L.G. Maksimova, *J. Struct. Chem.* 44, 180 (2003).
- [16] H. Yu, X. Zhang, A.F. Jalbout, X. Yan, X. Pan, H Xie, R. Wang, *Electrochimica Acta*, 53, 4200 (2008).
- [17] K.-C. Hsiao, S.-C. Liao, J.-M. Chen, *Electrochim. Acta*, 53, 7242 (2008).
- [18] K.Q. Ding, T. Okajima and T. Ohsaka, *Electrochemistry*, 75, 35 (2007).
- [19] A.Y. Shenouda, K.R. Murali, *J. Power Sources*, 176, 332 (2008).
- [20] M.-R. Yang, T.-H. Teng, S.-H. Wu, *J. Power Sources*, 159, 307 (2006).
- [21] G.T.-K. Fey, Y.G. Chen, H.-M. Kao, *J. Power Sources*, 189, 169 (2009).
- [22] Wei-Jun Zhang, *J. Power Sources*, 196, 877 (2011).
- [23] A.N. Jansen, A.J. Kahaian, K.D. Kepler, P.A. Nelson, K. Amine, D.W. Dees, D.R. Vissers, M.M. Thackeray, *J. Power Sources*, 81, 902 (1999).